Characterization of PVA cryogel for intravascular ultrasound elasticity imaging

J. Fromageau, E. Brusseau, D. Vray, G. Gimenez, Philippe Delachartre

Characterization of PVA Cryogel for Intravascular Ultrasound Elasticity Imaging

Jérémie Fromageau, Elisabeth Brusseau, Didier Vray, *Member, IEEE*, Gérard Gimenez, *Member, IEEE*, and Philippe Delachartre

***Abstract*—The present study characterizes the mechanical properties of polyvinyl alcohol (PVA) cryogel in order to show its utility for intravascular elastography. PVA cryogel becomes harder with an increasing number of freeze-thaw cycles, and Young's modulus and Poisson's ratio are measured for seven samples. Mechanical tests were performed on cylindrical samples with a pressure column and on a hollow cylinder with the calculation of an intravascular elastogram. An image of the Young's modulus was obtained from the elastogram using cylinder geometry properties. Results show the mechanical similitude of PVA cryogel with the biological tissues present in arteries. A good agreement between Young's modulus obtained from pressure column and from elastogram was also observed.**

I. Introduction

Since palpation detects pathological areas, estimating and mapping tissue stiffness is of interest to medical diagnosis. Over the last ten years, many studies using ultrasound have made it possible to identify abnormalities too small or too deep to be detected by palpation. Several approaches have been discussed in the literature most based on two concepts: sonoelasticity, investigating the response of tissues to a low frequency wave, where the induced displacement is measured by Doppler ultrasound [1] and elastography, where the displacement is determined by time-delay estimation methods between the signal at a low compression level and the signal at a high compression level [2], [3]. More recently, elastography has been used in combination with intravascular techniques in view of characterizing elastic properties of atherosclerotic plaque and vessel walls [4]–[7]. Combining high-resolution imaging with deformation estimation techniques may provide useful information for characterizing plaque and predicting progression.

Validation requires conducting experiments on test objects. Indeed working on phantoms is convenient since parameters of the studied object, such as the geometry and number of layers are precisely controlled. Commonly the material used to build phantoms is a mixture of gelatin and agar [8]. These phantoms accurately mimic the acoustical properties of biological tissues as well as their incompressible character; however, without a cross-linking step they crack easily with increasing pressure [9]. Polyvinyl alcohol (PVA) cryogel is another kind of material with the ease-of-handling properties of gelatin-agar, which seems well adapted for intravascular elastography. It is a material initially used for mimicking blood vessels in *in vitro* MRI experiments [10]. Its acoustic properties have been proved to be similar to those of arteries. The speed of sound has a mean value of 1538 ms^{-1}, with a range of 1530 to 1545 ms^{-1} and a slight increase of 5 ms^{-1} for each new freeze-thaw cycle [11]. Acoustic impedance is 1.6×10^6 kg m^{-2} s^{-1} and attenuation around 0.6 $dBcm^{-1}$ MHz^{-1} measured at 5 MHz [12]. These values can be compared with those reported by Greenleaf for arterial tissues of several lesions: sound velocity between 1501 and 1532 ms^{-1}, acoustic impedance from 1.56 to 1.69 10^6 kg m^{-2} s^{-1}, and attenuation between 0.6 and 1.5 $dBcm^{-1}$ MHz^{-1} measured at 10 MHz [13]. However, it is desirable to have a precise mechanical characterization of this potentially usable material. In this article, we describe the fabrication of phantoms and the devices used for their mechanical characterization. This characterization is done in two ways: with a pressure column first and then with the calculation of an intravascular ultrasound elastogram. This will make it possible to calibrate the intravascular stiffness image by comparing Young's modulus obtained both ways. Finally, we present the results and compare them with values reported in literature.

II. Methods

A. Building Procedure

The PVA cryogel solution is a viscous liquid composed of 10% of polyvinyl alcohol dissolved in water. Preparation consists of heating PVA cryogel, mixing it with silica powder in a 1% by weight concentration (Prolabo Silicagel, impalpable powder) and then freezing it. Silica particles act as acoustic scatterers and have been introduced to generate images with a sufficient signal-to-noise ratio. As a cryogel, this material gets its rigidity by a freeze-thaw process, its stiffness increasing with the number of freezing cycles. For this study, two kinds of samples were made: 1) a full cylinder for measuring elasticity with a pressure column and 2) a hollow cylinder to be investigated using elastography. To have the same material properties for both tests, we made both samples in the same mold, and, after the last freeze cycle, we cut the cylinder into two pieces, a

hollow and a full part. Two samples were built with three and four freeze-thaw cycles, and two samples were built with two cycles to check reproducibility. One cycle consisted in 14 h of freezing at −20°C and 10 h of thawing in water at 20°C. Three additional samples were built changing the cycle. The cycle duration was maintained constant (14 h of freezing and 10 h of thawing), but the freezing rate decreased to −32°C. One of these three samples was made with five freeze-thaw cycles and the two other ones with two cycles. During the building procedure, dehydration was minimized by covering the container.

B. Measurement of Mechanical Properties

1. Measurement with Pressure Column: Young's modulus was measured using an Instron 4301 testing instrument. The cryogel samples were 12-mm-diameter cylinders whose heights varied according to the sample, due to the difficulty in cutting PVA cryogel precisely. The load cell was rated at 10 N with an accuracy of 0.05 N. The diameter of the cell was 25 mm, thus larger than the sample radius in the aim to approximate the conditions of uniform stress. The samples were tested for pressure in the range 0 to 5 N. Measurements were taken dynamically, with two steps of compression per second, one step corresponding to a displacement of 0.05 mm. A precompression of 0.1 N was initially applied to the sample to insure proper contact. Owing to the radius of the sample, a force of 2 N corresponded to a stress of about 100 mmHg. Thus, the samples were tested on a range including the physiological pressure of arteries.

Poisson's ratio was also estimated from two digital pictures of one sample. The first image corresponded to the sample before compression and gave the apparent area of the cylinder S_O. The apparent area was a rectangle whose size is given by the diameter and the height of the cylinder. The second image corresponded to the sample after compression and gave the apparent area of the cylinder S_F. The area difference $\triangle S$ is related to Poisson's ratio by the expression:

$$\triangle S = S_F - S_O = (\nu - 1)\varepsilon S_O \tag{1}$$

where ν is Poisson's ratio and ε the axial deformation. Note that for an incompressible material ($\nu = 0.5$), there is no change in volume ($\triangle V = 0$), but there is a variation in area ($\triangle S \neq 0$) in (1).

2. Measurement with Ultrasound: On the other hand, Young's modulus was measured using intravascular cryogel phantoms. The geometrical characteristics of the hollow cylinders used in this study were a 2.5-mm inner radius, a 6-mm outer radius and a length larger than 60 mm. Furthermore, each sample was considered homogeneous and isotropic, and its rigidity resulted from two, three, four, or five freeze-thaw cycles. For a cylinder with an axial symmetry, the radial displacement and radial strain can be written as [14]

$$u_r(r) = \frac{A}{r} + Br \tag{2}$$

$$\varepsilon_{rr} = \frac{\partial u_r}{\partial r} = -\frac{A}{r^2} + B \tag{3}$$

Considering a homogeneous and isotropic hollow cylinder with outer boundaries radially fixed and a load applied on the internal boundary, the boundary conditions are

$$\sigma_{rr}(a) = \frac{E}{1+\nu}\left(-\frac{A}{r^2} + B\frac{1+\nu}{1-\nu}\right) = -P \tag{4}$$

$$u_r(b) = 0 \tag{5}$$

where a is the inner radius, b the outer radius, E Young's modulus, ν Poisson's ratio, and P the pressure into the phantom lumen. Including boundary conditions (5) in (3), Young's modulus is calculated by the radial strain

$$E = \frac{-Pa^2(1-\nu^2)}{\varepsilon_{rr}(r)(b^2(1-\nu) + a^2(1+\nu))}\left(1 + \frac{b^2}{r^2}\right) \tag{6}$$

where ε_{rr} is the radial strain. Using relation (6) and the elastogram as the strain distribution, an image of Young's modulus is obtained.

The experimental setup consisted of a CVIS (Boston Scientific, Natick, MA) ultrasound scanner, working with a 40-MHz mechanically rotating single-element transducer. The catheter was inserted inside the lumen phantom. The probe was fixed approximately at the center of the lumen and parallel to the lumen axis to limit geometrical artifacts [15] and correlate the direction of the ultrasound beam and force lines. Thus, the calculated elastogram effectively represented the radial deformation. The phantom was clamped at the extremities to ensure that the device is watertight. The phantom was embedded in a plexiglas mold, then radial displacement of the outer boundary was not allowed because of the high stiffness contrast between the mold and the phantom; nevertheless, the phantom could expand in the axial direction, resulting in a radial strain. The inner pressure variation was manually generated by increasing or decreasing the fluid lumen volume via a syringe and varied from 0 mmHg to 160 mmHg. Static pressure was accurately controlled by a surgery manometer. For each acquisition, a 256-line scan was performed. The RF signals were acquired via a LECROY 9374L oscilloscope at the sampling frequency of 500 MHz in an 8-bit format. Radial deformation was estimated with an adaptive stretching algorithm, which has been proved to be accurate for strains up to 7% [6]. Using (1) and (6), the value of Young's modulus was deduced for each sample.

III. Results

From the experiments with the pressure column, applied stress data and induced strain data are available.

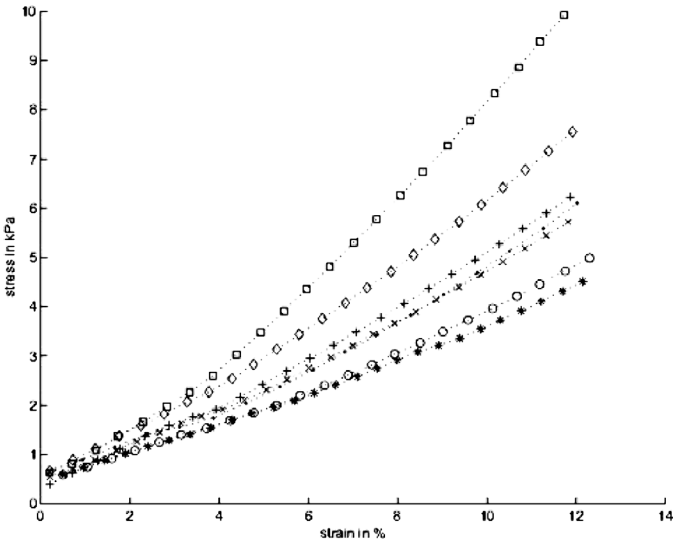

Fig. 1. Strain-stress relation obtained from pressure column for samples with different numbers of freeze-thaw cycles: □ 5 cycles, ◇ 4 cycles, ■ 3 cycles, ○ and ∗ 2 cycles at −20°, + and × 2 cycles at −32°. Young's moduli are calculated as the slopes of segment on three dots, a range where the curves can be approximated to straight lines.

The strain-stress curve is plotted for each cryogel sample on Fig. 1.

According to Hooke's law, a Young's modulus can be measured for each compression step, calculating the corresponding slope on the strain-stress curve.

$$\sigma_{zz} = E_i \varepsilon_{zz} \tag{7}$$

On each curve, slopes are calculated from a segment made of three consecutive points. Young's moduli of each sample are deduced from the mean of these slopes, $\overline{E}$, and their linearity deviation σ_E^2

$$\begin{aligned} \overline{E} &= \frac{1}{K}\sum_{i=1}^{K} E_i \\ \sigma_E^2 &= \frac{1}{K}\sum_{i=1}^{K}(E_i - \overline{E})^2, \end{aligned} \tag{8}$$

where K is the number of Young's modulus estimated for each sample, and $K+2$ is the number of points on the corresponding curve.

The results show that Young's modulus values are in the range [30 kPa to 100 kPa]. The exact values $\overline{E} \pm \sigma_E$ are reported on Table I. Each category of phantom has a well-discriminated stiffness, represented on Fig. 1 by a gap between two curves. Only one exception can be observed: the Young's modulus of the sample subjected to three freeze-thaw cycles at −20°C, and those of the sample that underwent two cycles at −32°C are fairly close (curves ■, +, and ×). This demonstrates the importance part of the freezing rate. However, for two samples built following an identical process and different in only one freeze-thaw cycle, the modulus difference is relatively constant and significant, about 15 kPa.

TABLE I
MEAN YOUNG'S MODULUS AND POISSON'S RATIO FOR PVA CRYOGEL MEASURED FROM THE PRESSURE COLUMN.

Number of freeze-thaw cycles	Young's Modulus in kPa	Poisson's ratio
5 cycles (−32°C)	89.1 ± 6.3	0.48 ± 0.03
4 cycles (−20°C)	61.0 ± 9.0	0.43 ± 0.02
3 cycles (−20°C)	55.3 ± 12.6	0.45 ± 0.03
2 cycles (−32°C)	51.2 ± 9.2	0.42 ± 0.02
2 cycles (−20°C)	42.8 ± 8.0	NC

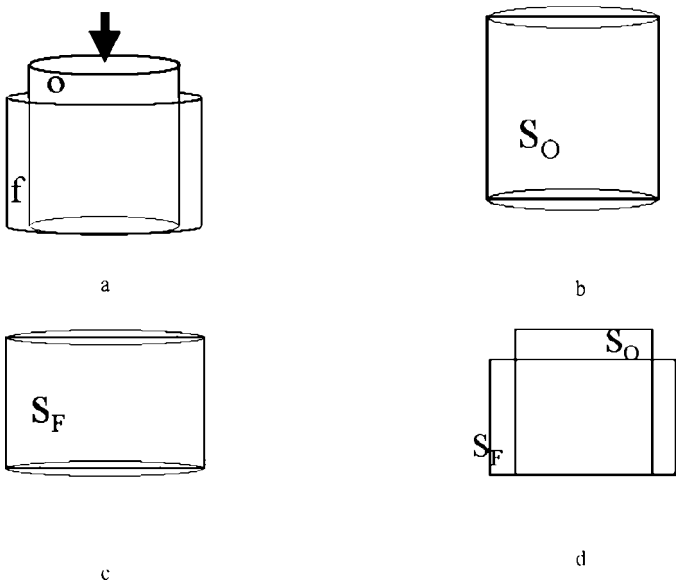

Fig. 2. Estimation of the Poisson's ratio. (a) Original sample ○ is compressed to the final shape f. (b) Sample before compression, the initial surface S_O is estimated. (c) Sample after compression S_F is estimated. (d) The variation of area $\triangle S = (S_O - S_F)$. The Poisson's ratio is then estimated from this area variation.

A first investigation of reproducibility was studied with samples at two freeze-thaw cycles. In both cases we observed a slight difference, less than 1 kPa for the samples with cycles at −32°C and a few kilipascals for samples with cycles at −20°C. The difference probably arises from steps in the building procedure, which were not exactly the same for all samples. Especially after having poured the solution in the mold, it was left to rest to allow bubbles to rise. During this period, a little dehydration can occur, significantly influenced by atmospheric conditions. To have a better match, these steps must be carried out with particular care. Nevertheless, the variance between two samples, which underwent the same building procedure, was acceptable for our application. In the literature, reported radial Young's moduli are around 80 kPa for the healthy adventicia, 10 kPa for the healthy media, 50 kPa for mixed fibrosis, 20 kPa for cellular fibrosis, and 100 kPa for dense fibrosis [16]. In another reference, tissues were classified from their intravascular ultrasound appearance; stiffnesses reported are 40 kPa and 80 kPa for nonfibrous and fibrous classes respectively [17].

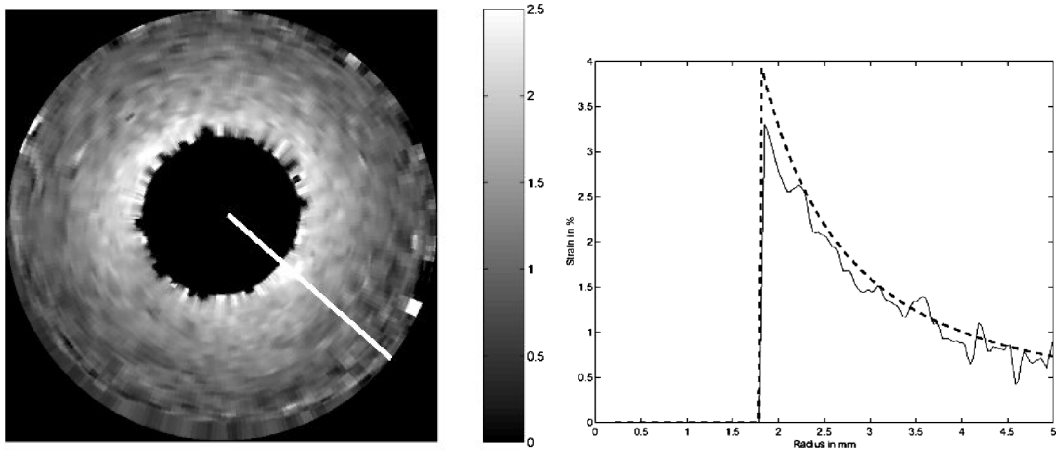

(a) Elastogram and strain profiles

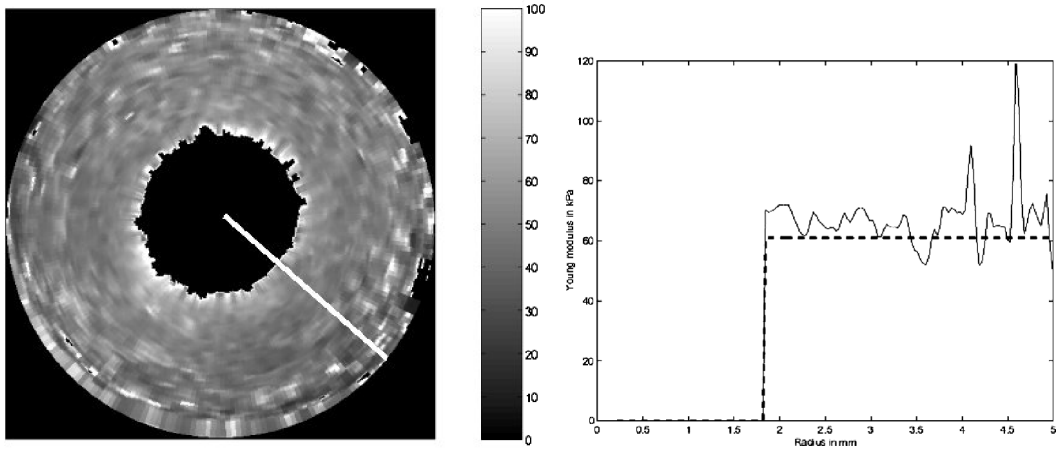

(b) Young's modulus image and profiles

Fig. 3. (a) Elastogram, reference strain profile (dotted line), and estimated strain profile (solid line) (b) Young's modulus image, reference profile (dotted line), and estimated profile (solid line) obtained for a 4 freeze-thaw cycles homogeneous phantom with a pressure differential of 10 mmHg. Young's modulus measured on column pressure is the reference. The Young's modulus image is calculated from the elastogram. Profiles are plotted for a line (white line on images), which have a good mismatch with measured value. Note on the Young's modulus profile that the decrease due to cylindrical geometry is compensated.

To estimate Poisson's ratio, samples were compressed by a plate, digital pictures were made at each compression step, and the area variations were measured from the pixels of the images after a segmentation processing using a manual thresholding. The plate displacement step was 0.5 mm. From (1), Poisson's ratio is given by

$$\hat{\nu} = 1 + \frac{\Delta S}{\epsilon S_O} \tag{9}$$

where $\Delta S = S_O - S_F$ is the area variation, calculated as shown in Fig. 2. Results obtained for Poisson's ratio show that values reported on Table I are close to the incompressible case, ranging from 0.42 to 0.48. Poisson's ratio was not calculated for the very soft sample, because of its imperfect cylinder shape under compression. Measurement of Poisson's ratio error depends on measurement errors expressed by

$$\text{error}(\hat{\nu}) = \frac{1}{1 + \frac{\epsilon S_O}{\Delta S}} \left[\text{error}(\Delta S) + \text{error}(\epsilon) + \text{error}(S_O)\right] \tag{10}$$

where ϵ is the measured axial strain, S_O the area of the sample before compression, and ΔS the area variation between two steps of compression. All errors are related to measurement on the picture and the ability to distinguish the phantom from the background on the image. Due to the boundaries, accuracy errors are estimated at 2% on the area and the area variation and 1% on the axial strain. This implies an error of about 5% on the Poisson's ratio value.

The last step of the calibration is the calculation of an image of Young's modulus via the elastogram, Fig. 3(a). This image is obtained from (6). It is necessary to determine the inner and outer radius of the phantom boundaries, a and b, and also the radial deformation ε_{rr}, which is the resulting elastogram. Thus we deduce an image of a quasi-constant parameter, which is the Young's modulus on Fig. 3(b). On the same figure, the radial strain profile and the radial Young's modulus profile are plotted. The result we show on Fig. 3 is for a phantom, which underwent four freeze-thaw cycles. Estimated strain and Young's modulus profiles are plotted for one of the line (white line

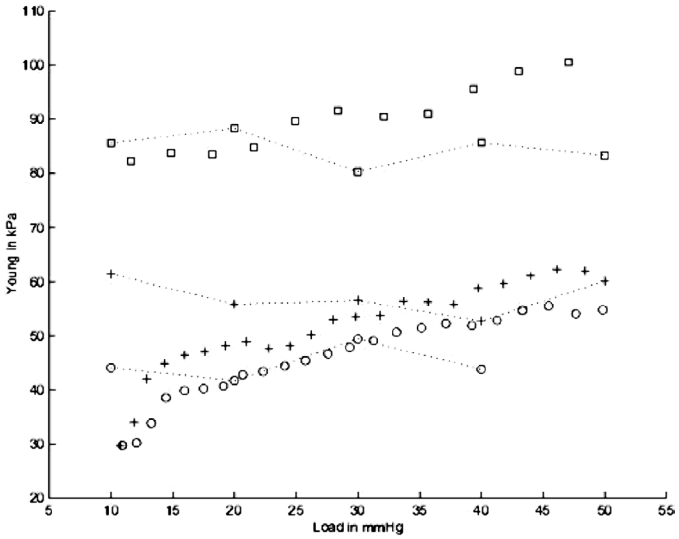

Fig. 4. Mean Young modulus measured by elastography (dotted lines) and pressure column (marks) for different compression steps on 3 samples with different numbers of freeze-thaw cycles: □ 5 cycles, ○ 2 cycles at −20°, + 2 cycles at −32°.

on images), which has the best mismatch with the reference profiles. The reference profile for the Young's modulus is the value measured with the column pressure, 61 kPa, and the reference profile of strain is mathematically deduced from (6) with this value of Young's modulus. For comparison mean, Young's modulus was measured with column pressure at 61 kPa, whereas the estimated value from ultrasound intravascular elastography for this profile is around 70 kPa. In the radial strain profile, a decrease can be observed in the strain magnitude induced by the decay of the stress when propagating across the phantom wall. On the other hand, this phenomenon is compensated when reconstructing Young's modulus.

These images are calculated for each phantom at different steps of compression. Stress-Young's modulus curves are plotted (dotted lines Fig. 4) for some samples and for loads in the order of magnitude of physiological overloads. Young's modulus is nearly constant for the low loads, but a slightly increased behavior is observed. On the same figure, results obtained from the pressure column are plotted (marks Fig. 4). The results are correlated to their global behavior but with a difference of about 10% for numerical values of mean Young's moduli, Table II. The linear model of elasticity is no more valid for high deformations, over 20%, corresponding to a pressure value of 50 mmHg for the softer sample. This may be due to the reach of nonlinear behavior of the medium. For this reason, the mean Young's modulus is estimated only for loads smaller than 50 mmHg.

The mean Young's moduli calculated from experimental images are recorded on Table II.

The mean is calculated from results obtained for different loads. The Young's modulus estimated using the ultrasonic method are for the most part higher than the Young's modulus measured from the pressure column. The most important sources of error are related to differences with the theoretical model, which tend to underestimate the strain. Parameters, such as a badly centered probe, which caused a mismatch of force lines and ultrasound beams [18] and damping of the stress propagation, give a calculated strain lower than the expected strain and lead to overestimating the Young's modulus. However, estimated mean Young's moduli are similar to the values found by the way of the column pressure and to the values of biological tissues edited previously.

TABLE II
Comparison of Measured Mean Young's Modulus for PVA Cryogel for Each Method. The Mean Young's Modulus is Calculated Over the Stress Range 0 to 50 mmHg.

Number of freeze-thaw cycles	Young's Modulus from pressure column experiment	Young's Modulus from ultrasonic method
5 cycles (−32°C)	89.1 kPa	84.6 kPa
4 cycles (−20°C)	61.0 kPa	66.4 kPa
3 cycles (−20°C)	55.3 kPa	59.4 kPa
2 cycles (−32°C)	51.2 kPa	57.3 kPa
2 cycles (−20°C)	42.8 kPa	44.8 kPa

IV. Conclusion

In this paper we have measured the mechanical properties of PVA cryogel for building phantoms in intravascular elastography. The cryogel mechanical properties, as function of the number of freeze-thaw cycle, have been evaluated for an over-pressure range from 0 to 50 mmHg by two different methods. First, the Young's modulus and the Poisson's ratio were measured using a pressure column, and second, the Young's modulus was deduced from the calculation of an ultrasound elastogram. The Young's modulus calculated with the two methods are in a range of 40 to 90 kPa, which is in the same range as arterial tissues described in the literature, 10 to 100 kPa. The experimental results emphasize the interest of PVA cryogel as vascular phantoms for intravascular ultrasound elastography.

Acknowledgments

The authors would like to thank Sandrine Dorthe from Cermav Grenoble for her help in the pressure column experiments and Mrs. Macovschi and Mr. Savany from the Laboratoire de biochimie et Pharmacologie for providing the freezer required for building the phantom.

References

[1] R. M. Lerner, S. R. Huang, and K. J. Parker, "Sonoelasticity images derived from ultrasound signals in mechanically vibrated tissues," *Ultrasound Med. Biol.*, vol. 16, no. 3, pp. 231–239, 1990.

[2] J. Ophir, I. Cespedes, H. Ponnekanti, Y. Yasdi, and X. Li, "Elastography: A quantitative method for imaging the elasticity of biological tissues," *Ultrason. Imag.*, vol. 13, no. 2, pp. 111–134, 1991.

[3] K. S. Alam, J. Ophir, and E. E. Konofagou, "An adaptive strain estimator for elastography," *IEEE Trans. Ultrason., Ferroelect., Freq. Contr.*, vol. 45, no. 2, pp. 465–472, 1998.

[4] B. M. Shapo, J. R. Crowe, A. R. Skovoroda, M. J. Eberle, N. A. Cohn, and M. O'Donnell, "Displacement and strain imaging of coronary arteries with intraluminal ultrasound," *IEEE Trans. Ultrason., Ferroelect., Freq. Contr.*, vol. 43, no. 2, pp. 234–246, 1996.

[5] C. L. de Korte, E. I. Cespedes, A. F. W. van der Steen, and C. T. Lancee, "Intravascular elasticity imaging using ultrasound: Feasibility studies in phantoms," *Ultrasound Med. Biol.*, vol. 23, no. 5, pp. 735–746, 1997.

[6] E. Brusseau, C. Perrey, P. Delachartre, M. Vogt, D. Vray, and H. Ermet, "Axial strain imaging using local estimation of the scaling factor from RF ultrasound signals," *Ultrason. Imag.*, vol. 22, no. 2, pp. 95–107, 2000.

[7] J. Fromageau, P. Delachartre, R. El Guerjouma, J. C. Boyer, and G. Gimenez, "Modelling and measurement of cryogel elasticity properties for calibrating of IVUS elasticity images," *Proc. IEEE Ultrason. Symp.*, San Juan, Puerto Rico, Oct. 22–25, 2000, vol. 2, pp. 1817–1820.

[8] C. L. de Korte, E. I. Cespedes, A. F. W. van der Steen, C. van Birgelen, and K. te Nijenhuis, "Elastic and acoustic properties of vessel mimicking material for elasticity imaging," *Ultrason. Imag.*, vol. 19, no. 2, pp. 112–126, 1997.

[9] L. K. Ryan and F. S. Foster, "Tissue equivalent vessel phantoms for intravascular ultrasound," *Ultrasound Med. Biol.*, vol. 23, no. 2, pp. 261–273, 1997.

[10] K. C. Chu and B. K. Rutt, "Polyvinyl alcohol cryogel: An ideal phantom material for MR studies of arterial flow and elasticity," *Magnetic Resonance in Medecine*, vol. 37, no. 2, pp. 314–319, 1997.

[11] K. J. M. Surry, C. C. Blake, K. C. Chu, M. Gordon, B. K. Rutt, A. Fenster, and T. M. Peters, "Poly(vinyl alcohol) phantoms for use in MR and US imaging," *Medical Physics*, vol. 25, no. 44, pp. 1082–1083, 1998.

[12] M. Nambu, T. Watari, T. Sakamoto, and K. Akojima, "Method for applying electromagnetic wave and ultrasonic wave therapies," U.S. Patent No. 4958626, Sep. 25, 1990.

[13] J. F. Greenleaf, F. A. Duck, W. F. Samayo, and S. A. Johnson, "Ultrasonic data acquisition and processing system for atherosclerotic tissue characterisation," in *Proc. IEEE Ultrason. Symp.*, 1974, pp. 738–743.

[14] L. Landau and E. Lifchitz, "Course of theoretical physics, Theory of elasticity," *Mir Editions*, vol. 7, 1990.

[15] P. Delachartre, C. Cachard, G. Finet, L. Gerfault, and D. Vray, "Modeling geometric artefacts in intravascular ultrasound imaging," *Ultrasound Med. Biol.*, vol. 25, no. 4, pp. 567–575, 1999.

[16] H. M. Loree, R. D. Kamm, R. G. Stringfellow, and R. T. Lee, "Effect of fibrous cap thickness on peak circumferential stress in model atherosclerotic vessels," *Circ. Res.*, vol. 71, no. 2, pp. 850–858, 1992.

[17] R. T. Lee, S. G. Richardson, H. M. Loree, A. J. Grodzinsky, S. A. Gharib, F. J. Schoen, and N. Pandian, "Prediction of mechanical properties of human atherosclerotic tissue by high frequency intravascular ultrasound imaging. An in vitro study," *Arteriosclerosis, Thrombosis and Vascular Biology*, vol. 12, pp. 1–5, 1992.

[18] C. L. de Korte, E. I. Cespedes, and A. F. W. van der Steen, "Influence of catheter position on estimated strain in intravascular elastography," *IEEE Trans. Ultrason., Ferroelect., Freq. Contr.*, vol. 46, no. 3, pp. 616–625, 1999.

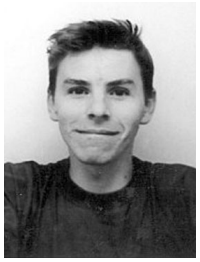

Jérémie Fromageau was born in Orléans, France, in 1975. He received his M.Sc. degree in physical acoustic at the University Denis Diderot, Paris 7, in 1999. He is currently working toward a Ph.D. degree in medical image processing at CREATIS. CREATIS is a research unit of the French National Center for Scientific Research (CNRS), common to INSA-Lyon and University Claude Bernard-Lyon. His research interests include signal and image processing applied to medical ultrasound imaging and elastography.

Elisabeth Brusseau was born in Gien, France, in 1973. She received her Dipl.-engineerer and M.Sc. degree in biomedical engineering from the Technological University of Compiègne, France, in 1997. She received a Ph.D. in medical imaging in the CREATIS laboratory. She more precisely worked in ultrasound elastography. In 2001, she completed a postdoctoral training period at the experimental echocardiography directed by A.F.W. Van der Steen in Rotterdam, the Netherlands, where she worked on contour detection. She is now a CNRS researcher at the CREATIS laboratory, and her research focuses on ultrasound elastography to investigate the mechanical properties of carotid arteries. Her research interests are signal and image processing, medical imaging, elastography, and ultrasounds.

Didier Vray (M'92), was born in Saint-Etienne, France, in 1959. He received a Ph.D. degree from the Institut National des Sciences Appliquées (INSA), Lyon, France, in 1989. He is currently Professor of signal processing and computer sciences at INSA de Lyon. Since he joined the research laboratory CREATIS, his main research interests are ultrasound medical imaging, elastography, and high frequency imaging.

Gérard Gimenez (M'92) received his M.Sc. degree from the University of Lyon in 1970, his Doctorat from the University of Marseille in 1972, and his Ph.D. degree from the University of Paris-Sud Orsay in 1978. He has been with CREATIS, a joint laboratory of the Centre National de la Recherche Scientifique (CNRS), the Institut National des Sciences Appliquées de Lyon (INSA Lyon), and the University Claude Bernard Lyon 1 since 1980. His research interests are in the field of image and signal processing, particularly involving interaction between ultrasound and biological tissues. He was a member of the Technical Committee of the IEEE Ultrasonics Symposium from 1994 to 2000.

Involved in the management of CREATIS since 1992, he was the director of the lab between 1995 and 2001. Since 2001, he is director of Centre d'Exploration et de Recherche Médicales par Emission de Positons (CERMEP), a PET imaging center in Lyon. CERMEP is currently evolving toward a multimodalities imaging facility for man and animal. He is currently a professor with the Electrical Engineering Department at INSA Lyon.

Philippe Delachartre received in 1990 his M.S. degree and in 1994 a Ph.D. degree, both in Signal and Image Processing in Acoustics from the National Institute for Applied Sciences of Lyon (INSA-Lyon, France). Since 1995, he has worked as an associate professor at the Electrical Engineering department of the National Institute of Applied Sciences of Lyon, France, and researcher at the Center for Research and Applications in Image and Signal Processing (CREATIS). His research interests include the image formation modeling and the parametric imaging applied to the field of medical ultrasound imaging.